

A pseudo-breakup observation: Localized current wedge across the postmidnight auroral oval

N. Partamies

Geophysical Research, Finnish Meteorological Institute, Helsinki, Finland
 Department of Physics, University of Helsinki, Helsinki, Finland

O. Amm, K. Kauristie, T. I. Pulkkinen, and E. Tanskanen

Geophysical Research, Finnish Meteorological Institute, Helsinki, Finland

Received 23 January 2002; revised 30 April 2002; accepted 28 May 2002; published 15 January 2003.

[1] This study presents a detailed description and analysis of a pseudo-breakup, which took place in the field of view (FOV) of the Magnetometers–Ionospheric Radars–All-sky Cameras Large Experiment (MIRACLE) network (IMAGE magnetometers, Scandinavian Twin Auroral Radar Experiment [STARE] radars, and all-sky cameras) on 3 November 1997 at 2212 UT. The activation lasted ~ 10 min, occurred during geomagnetically quiet conditions ($Dst \geq -10$ nT), and was followed by a global-scale substorm about half an hour later (at 2246 UT). Both the pseudo-breakup and the substorm had onsets at times corresponding to the Wind satellite observations of interplanetary magnetic field (IMF) B_Z northward turnings as delayed to the subsolar magnetopause. The auroral display of the pseudo-breakup was a mesoscale spiral with a counterclockwise winding direction. Simultaneously, STARE recorded clockwise plasma flow in the spiral surroundings. Applying the method of characteristics to the MIRACLE observations revealed that the spiral was associated with a localized current wedge (less than a few hours in MLT and about 4° in latitude), tilted in the northeast-southwest direction. The maximum upward current density at the western edge of the wedge was about 6 A/km^2 , which clearly exceeds the threshold of spiral buildup (2.5 A/km^2) suggested by earlier theoretical studies. About an hour before the pseudo-breakup, the energy input from the solar wind to the magnetosphere (quantified by the ϵ parameter) exceeded the substorm threshold and the ionospheric conductivity was high enough to support substorm activity. Two likely reasons for the activation to remain localized were its unfavorable location in the morning side of the Harang discontinuity region and the abrupt decrease of the solar wind energy input at its onset time. *INDEX TERMS*: 2407 Ionosphere: Auroral ionosphere (2704); 2437 Ionosphere: Ionospheric dynamics; 2784 Magnetospheric Physics: Solar wind/magnetosphere interactions; 2431 Ionosphere: Ionosphere/magnetosphere interactions (2736)

Citation: Partamies, N., O. Amm, K. Kauristie, T. I. Pulkkinen, and E. Tanskanen, A pseudo-breakup observation: Localized current wedge across the postmidnight auroral oval, *J. Geophys. Res.*, 108(A1), 1020, doi:10.1029/2002JA009276, 2003.

1. Introduction

[2] A pseudo-breakup is a small, localized substorm-like activation, which typically lasts less than 10 min and does not lead to a global reconfiguration of the magnetotail like substorms do. A pseudo-breakup typically precedes a full-scale substorm by some tens of minutes [Koskinen *et al.*, 1993; Cattell *et al.*, 1994]. In the literature, the definition of a pseudo-breakup often varies depending on the available observations. Some of the observations, without mentioning the term “pseudo-breakup”, carry the characteristics of what is now known to belong to a pseudo-breakup. Originally, the term was used to describe a highly localized (both

in space and time) auroral activation in the ionosphere, but later, with increasing availability of satellite observations, also localized magnetospheric activations were included in this definition.

[3] Despite being localized and short-lived, pseudo-breakups do not show any significant differences from substorm, either in the ionosphere or in the magnetosphere [e.g., Pulkkinen, 1996; Aikio *et al.*, 1999]. Thus, the trigger mechanism is expected to be similar for both kind of activations, and other properties must be in control of the size and duration of the event. Rostoker [1998] suggested that all auroral breakup activations are controlled by the same physics - no matter what the size is - and the substorm expansions are built up of a series of small-scale current systems, one of which could show up as a pseudo-breakup. In fact, the pseudo-breakup disturbances both in the plasma

sheet [Koskinen *et al.*, 1993; Pulkkinen *et al.*, 1998] and on the ground [e.g., Ohtani *et al.*, 1993] can also locally be of the same order of magnitude as the substorm onset-related disturbances. Pseudo-breakups can be associated with magnetic reconnection in the tail as well as a local dipolarization of the geomagnetic field, disruption of the tail current, dispersionless particle injections, and formation of a current wedge [Koskinen *et al.*, 1993; Nakamura *et al.*, 1994; Pulkkinen *et al.*, 1998]. Some pseudo-breakups have even been observed together with the ejection of a plasmoid [Aikio *et al.*, 1999].

[4] Pseudo-breakups have been observed in regions poleward [Akasofu, 1964] equatorward [Nakamura *et al.*, 1994] and westward [Amm *et al.*, 2001; Koskinen *et al.*, 1993; Ohtani *et al.*, 1993] of the following substorm activity. Vortex-like auroral structures (bulges, spirals, etc.) have often been recorded during pseudo-breakups [Nakamura *et al.*, 1994; Amm *et al.*, 2001] but, as reported by Partamies *et al.* [2001], auroral spirals per se do not imply a pseudo-breakup or any particular kind of magnetic activity. In the case studied here, a pseudo-breakup spiral was very clear and it was located poleward and eastward of the following substorm.

[5] The ionospheric and magnetospheric mechanisms preventing a pseudo-breakup from growing to a global-scale activation are still under discussion. At least three different possibilities have been suggested in the literature: insufficient energy flow from the solar wind to the magnetosphere, lack of stored energy in the tail [Nakamura *et al.*, 1994; Ohtani *et al.*, 1993; Amm *et al.*, 2001], or too low ionospheric conductivity to close the substorm current wedge [Koskinen *et al.*, 1993]. In this context, ionospheric feedback processes have to be taken into account because the travel time of the Alfvén waves (information) between the ionosphere and the magnetotail is about 1–5 min, which is of the order of the lifetime for pseudo-breakups [Pulkkinen, 1996].

[6] Amm *et al.* [2001] studied the ionospheric electro-dynamics of a pseudo-breakup event with the method of characteristics which provides a rigorous way to define the two-dimensional distribution of total ionospheric currents and conductivities. In their case, the conductivity in the analysis area appeared to be high enough for substorm activity and the current system was very similar to a substorm current wedge. Only western edge of the wedge, i.e., upward currents fed by westward currents, was found in the field of view of the instrumentation. The downward current part of the wedge was outside of the analysis region. The event of Amm *et al.* however, was not a typical pseudo-breakup as it was not followed by a substorm, but took place simultaneously with it in a region distinct from the main auroral bulge. In this study, we analyze a pseudo-breakup which clearly precedes a substorm. For this case, the method of characteristics yields an ionospheric current distribution different from the one reported by Amm *et al.* The global context of the event (interplanetary magnetic field [IMF] conditions and convection) is also discussed in more detail than in the previous study.

[7] In this paper, we briefly depict the instrumentation in section 2. In section 3 we describe both global and local observations. The observations are compared to previous pseudo-breakup studies in section 4, and conclusions are given in section 5, respectively.

2. Instrumentation

[8] This study utilizes the instrumentation of the Magnetometers–Ionospheric Radars–All-sky Cameras Large Experiment (MIRACLE) [Syrjäso *et al.*, 1998], i.e., the IMAGE magnetometer chain, FMI all-sky cameras (ASC), and Scandinavian Twin Auroral Radar Experiment (STARE). In 1997, IMAGE included 24 magnetometers with a latitude range from 59.90° to 78.92°. The IL index (local auroral electrojet (AL) index calculated from IMAGE) was used to characterize the intensity of the magnetic activity within the region covered by IMAGE. This index is defined as a lower envelope of the variations in the magnetic X-component at the IMAGE stations.

[9] The field of view (FOV) of an ASC covers a circular area with a diameter of about 600 km at the altitude of 110 km. This FOV of 140° corresponds to 440 pixels and thus, gives an average spatial resolution of a couple of km/pixel. The exact spatial resolution depends on the elevation angle, and is lower toward the horizon. Still, the resolution is better than 10 km/pixel everywhere. The images have been flipped in the east-west direction so that the auroras are viewed from above. Here we use ASC images from Muonio (MUO, 68.02°N and 23.53°E, or 64.65° CGM lat and 105.70° CGM lon) and Kilpisjärvi (KIL, 69.02°N and 20.87°E, or 65.81° CGM lat and 104.32° CGM lon) stations to study the evolution of both green (557.7 nm) and red (630.0 nm) auroras.

[10] The STARE radars [Greenwald *et al.*, 1978] are located at Hankasalmi in Finland and at Midsandn in Norway. They record coherent backscatter at the frequency of about 140 MHz. The FOV of STARE is a 400 km × 400 km rectangular area in the region 14°–26°E in longitude and 68°–73°N in latitude. The radar system measures the speed of meter-scale ionospheric irregularities in the E region at times when the electric field is larger than the threshold value of about 17 mV/m.

[11] We also show some data from the European Incoherent Scatter (EISCAT) UHF radar in Tromsø, Norway. This radar is operated at the frequency of 931 MHz, and a long pulse CP-1-k experiment was run on 3 November 1997 with the radar beam looking field-aligned.

[12] Solar wind parameters (magnetic field, velocity, pressure and density) were monitored by the Wind satellite at the distance of about 110 R_E from the Earth along the Sun–Earth line ($Y \approx -60 R_E$ and $Z \approx 15 R_E$ in GSE). Los Alamos National Laboratory (LANL) geostationary satellite LANL-97A provided energetic electron precipitation data, which can be used for monitoring the substorm activity in the Russian sector.

3. Data Description and Analysis

3.1. Solar Wind and Magnetospheric Conditions

[13] The first part of 3 November 1997, was geomagnetically quiet with the Dst index greater than -15 nT. The global AE index (not shown) indicated enhanced magnetic activity from around 1730 UT onward, and two activations of interest took place at 2212 UT and 2246 UT. According to the Wind satellite ($X_{GSE} \sim 110 R_E$), the IMF B_Z was positive at noon but started to decrease around 13 UT. After remaining negative (~ -4 nT) for several hours, the IMF B_Z

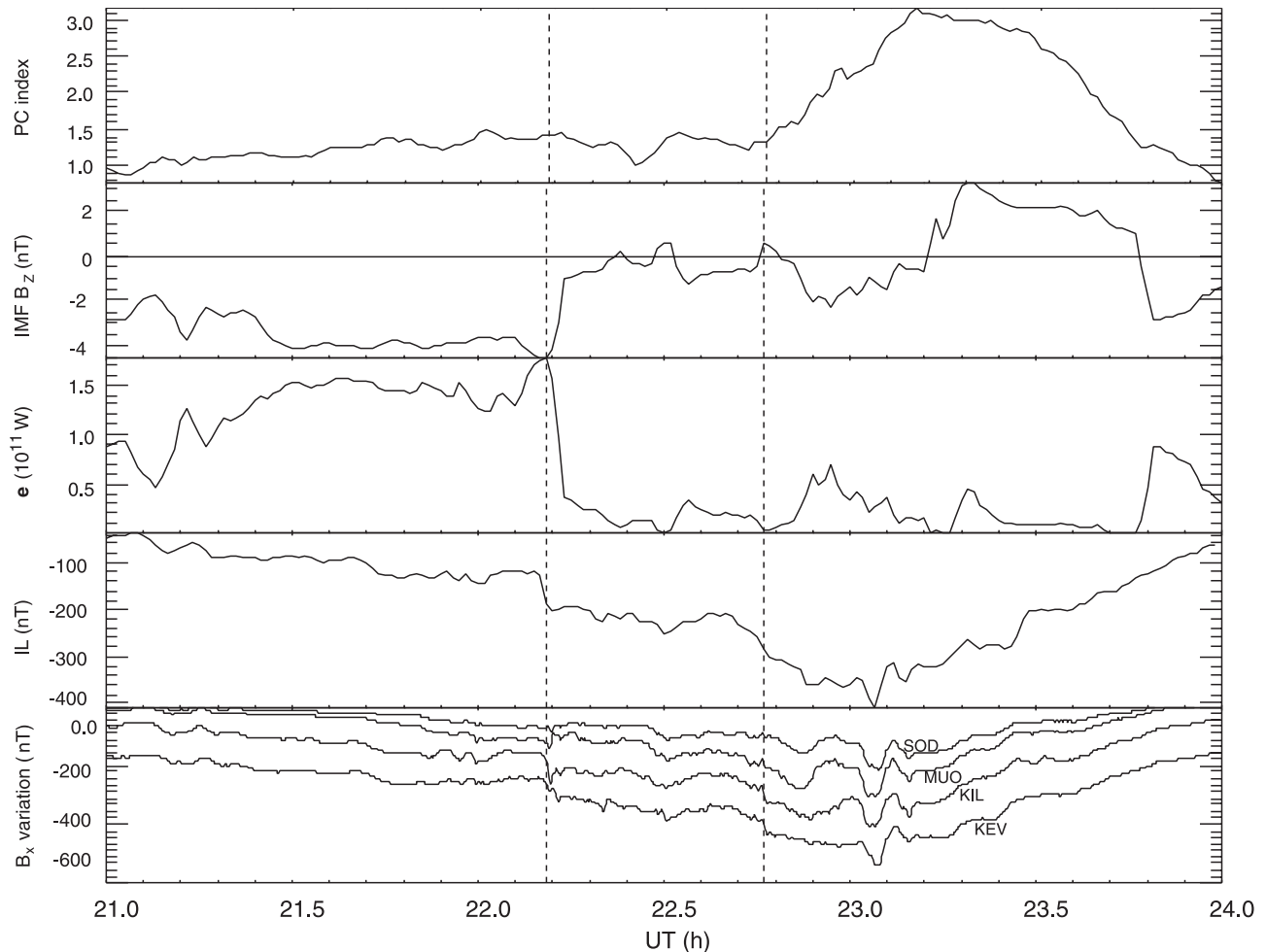


Figure 1. PC index (upper panel) shows the effect of the solar wind on the polar cap. IMF B_Z variations in GSE recorded by Wind satellite (second panel) shifted to the magnetopause with the time lag of 31 min. Epsilon parameter (third panel) shows the energy input from the solar wind shifted to the magnetopause. The IL index (fourth panel) describes the energy dissipation in the MIRACLE time sector. X-components of the magnetic field at SOD (67.37°N and 26.63°E or 63.92°MLAT and 107.26°MLON), MUO, KIL and KEV (69.76°N and 27.01°E or 66.32°MLAT and 109.24°MLON) are shown in the fourth panel. Vertical lines are drawn for the pseudo-breakup and the substorm onset.

suddenly increased by about 3 nT at 2141 UT (second panel in Figure 1) and simultaneous minor changes were observed in solar wind pressure and density. The third panel of Figure 1 shows the 1-min averaged ϵ parameter derived from the solar wind magnetic field data recorded by Wind according to the definition by *Perreault and Akasofu* [1978]. It had been at an elevated level for hours and became larger than the substorm threshold value of 10^{11} W [*Akasofu*, 1981] about an hour before the first activation. At 2141 UT the energy input from the solar wind to the magnetosphere suddenly decreased from $1.5 \cdot 10^{11}$ to $0.4 \cdot 10^{11}$ W. The time lag from the Wind location to the magnetopause was approximately 31 min according to the observed average solar wind speed (330 km/s). Thus, the northward turning and decrease in ϵ reached the magnetopause at the time of the first activation at 2212 UT (for caveats, see section 4.2). Simultaneously, the particle instrument onboard the Los Alamos National Laboratory (LANL) LANL-97A satellite (foot point at about 67°N and 70°E in geographical coordinates) recorded a drifting hole in the energetic

electron fluxes (lower panel in Figure 2). Similar holes have been observed at substorm onsets, they are of the same origin and occur simultaneously (but at higher energies) with the substorm related particle injections [*Sergeev et al.*, 1992].

3.2. Ionospheric Signatures

[14] The top panel in Figure 1 shows the northern polar cap (PC) index composed from the magnetic observations at THL station in Greenland [*Troshichev et al.*, 1979]. PC monitors the polar cap convection and is thus affected by both dayside and nightside merging rates. PC stayed around 1 mV/m during 2100–2230 UT despite the significant IMF B_Z changes. Only during the expansion phase of the substorm PC gradually increased to values ≥ 3 mV/m. Thus, THL seemed to monitor preferentially nightside reconnection effects and the IL index was more affected by the dayside reconnection.

[15] The IL index (in the fourth panel of Figure 1) shows two activations. The IMAGE magnetometer chain recorded

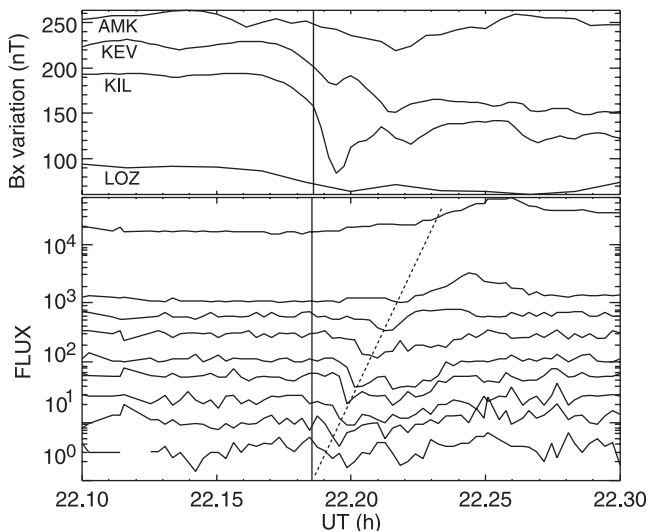


Figure 2. Variations of the B_x components from AMK, KEV, KIL and LOZ (upper panel, from west to east) show the longitudinal extent of the breakup region. Energetic electrons (lower panel, 50 keV–1.5 MeV, channels E1–E9) recorded by LANL-97A at the geosynchronous orbit. A dispersed drifting hole took place at 2212 UT.

the growth phase of the substorm as a gradual negative deviation in X . This means that the chain was below the morning sector westward electrojet. The pseudo-breakup at 2212 UT was observed as a ~ 50 nT disturbance in the growth phase trend simultaneously with the IMF B_z northward turning and geosynchronous drifting hole observations. The growth phase subsequently continued in the Scandinavian sector until an eastward expanding substorm activation reached the network at 2246 UT. The Greenland magnetometers in the evening sector (around 20 MLT) showed a small signature of the substorm onset at 2244 UT (data not shown). Neither CANOPUS (14–16 MLT) [Rostoker *et al.*, 1995] nor 210MM (~ 07 MLT) [Yumoto *et al.*, 1992] magnetometer chain recorded any signatures following the IMF B_z turning or substorm activity.

[16] A summary plot of the ionospheric measurements by the MIRACLE network and EISCAT Tromsø radar is shown in Figure 3. Both activations, the pseudo-breakup and the substorm (pink arrows and dashed lines), appear in the keogram (color-coded intensity in a latitude versus time plot, first panel) of the KIL all-sky camera as enhancements in luminosity. The pseudo-breakup auroras formed a spiral at the geographical latitude of 68.7° (65.3 in CGM), near the zenith of KIL. The following substorm onset appeared slightly southward of the geographical latitude of the pseudo-breakup. The boundaries of the westward electrojet (based on the variations in magnetic X component) plotted on the top of the keogram show that the activations appeared in the equatorward part of the westward electrojet. After 2300 UT the electrojet broadened due to the substorm expansion phase.

[17] The backscattered power measured by the STARE Norway radar (second panel) enhanced remarkably at 2212 UT. The strongest signals came from the latitudes north of the auroral emission, around 70° . At the substorm onset time (2246 UT), the backscatter region started to move

southward while the intensity of the signal remained at the same level.

[18] Prior to the pseudo-breakup, the EISCAT Tromsø radar recorded a clear decrease in the electron density (3rd panel). At the same time the ion temperatures (4th panel) were very high. This indicates that the radar measured strong electric field probably related to the pre-breakup arc south of the radar beam. According to the ASC images from KIL, the pre-breakup arc began to brighten at 2205 UT, which is also the time when the electron density decreased and the ion temperature enhanced. Shortly after 2212 UT, these conditions changed rapidly when the aurora reached the EISCAT beam causing an increased electron density layer to appear at the altitudes between 100 and 150 km.

[19] Only the riometers at Abisko (CGM lat 65.2), Kilpisjärvi (CGM lat 65.9) [Browne *et al.*, 1995], and Ivalo (CGM lat 65.0) of the 9-instrument network in Northern Scandinavia, Iceland and Svalbard (data not shown) recorded enhanced absorption associated with the activations. This suggests a localized source of energetic precipitation. The absorption peaks in the 1-min data coincided with the onsets of magnetic activations at 2212 UT and 2246 UT. The absorption peak of the pseudo-breakup was clearly shorter and less intense than that of the substorm onset. In both cases the enhancement was clearest at Abisko, which was located close to the region of the most

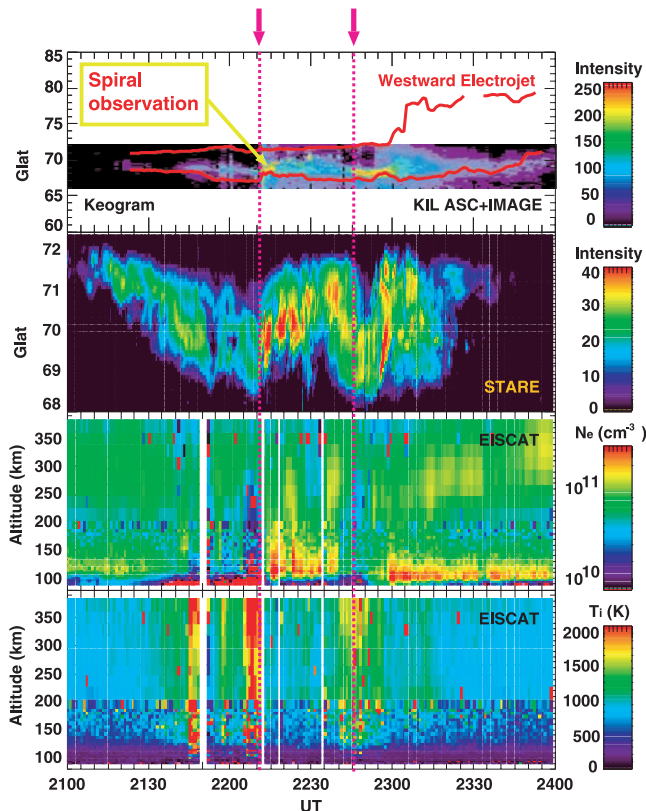


Figure 3. Ionospheric summary plot. First: KIL keogram with westward electrojet boundaries. Second: Signal-to-noise ratio from the STARE Norway radar. Third and fourth: Ion temperature and electron density from EISCAT Tromsø radar. Pink arrows and dashed lines mark the two activations.

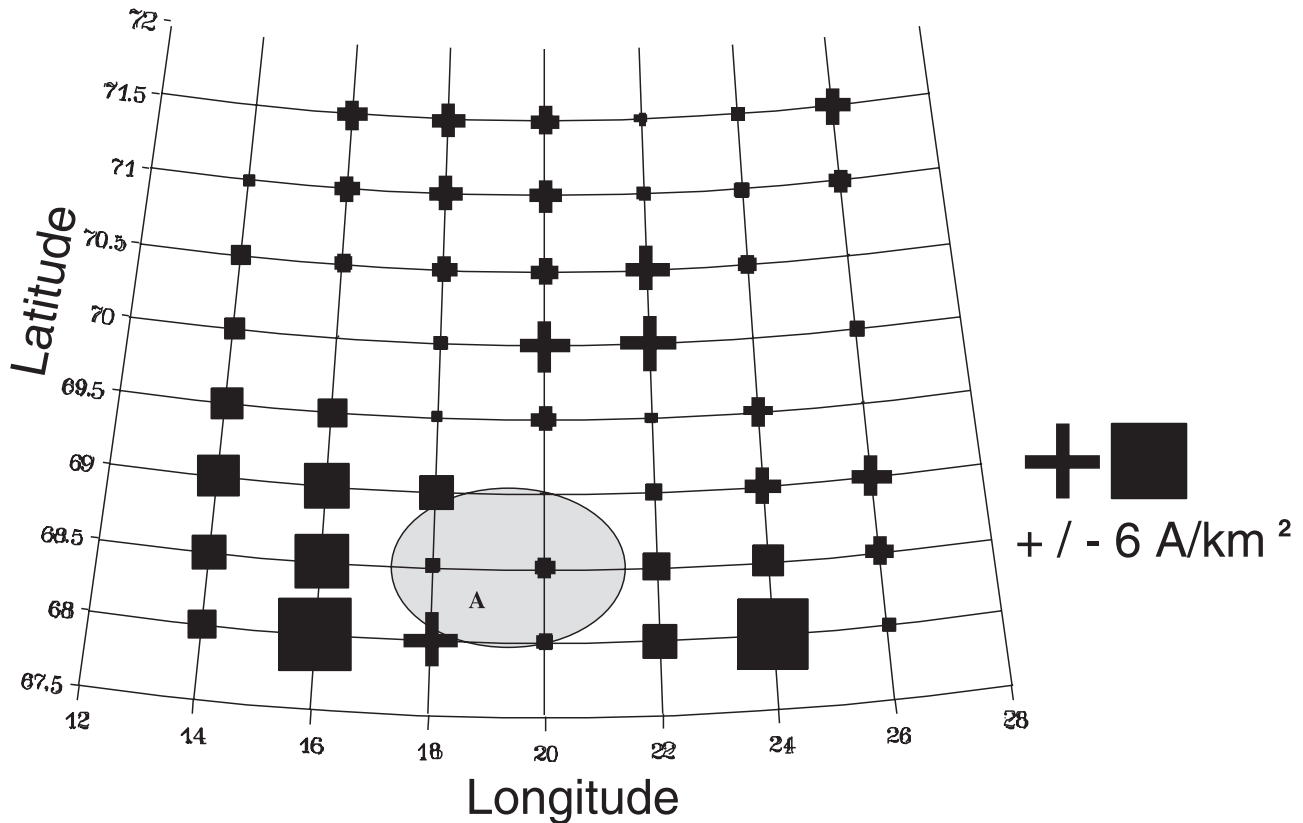


Figure 4. Distribution of the total upward (squares, negative) and downward (crosses, positive) FACs at 2212 UT derived from the method of characteristics. The shaded area marks the approximate location and size of the auroral spiral. The letter A shows the location of Abisko riometer.

intense upward FAC (see Figure 4). No drift motion is visible in the data as the peaks at this time resolution are simultaneous at all three stations.

[20] In the ASC images a quiet arc above both MUO and KIL brightened at 2205:00 UT, moved slowly southward and formed a street of 2 spirals. The first one was clearest at 2211:40 UT above MUO, while the other one was completely wound in the zenith of KIL at 2212:00 UT (top panel in Figure 5). The latter spiral was approximately twice as large (diameter over 300 km) as the first one and its evolution took roughly one minute. Afterward, the spiral broke and its remnants faded away, so that the sky was clear at 2216 UT in MUO and at 2220 UT in KIL.

[21] The images taken by the UVI imager on the Polar satellite [Torr *et al.*, 1995] (not shown) were available only for the last 1.5 hours of the day. The first UV image with an appropriate viewing angle was taken at 2225:51 UT, i.e., after the first activation but before the substorm onset. At this time, the oval over Scandinavia was very quiet. A few minutes later (at 2228:57 UT), VIS images showed a slightly broader and more active part of oval over Greenland. The next four UVI images (2235:03–2256:30 UT) illustrate how the region of substorm activity expanded to the MIRACLE MLT sector. The ASCs at MUO and KIL recorded a growth phase arc around 2243 UT but they did not show any significant activity after that.

[22] The longitudinal localization of the pseudo-breakup is demonstrated by Figure 2. The dispersed energetic electron hole is shown in the lower panel and the variations

of the magnetic X -components from AMK (Greenland east chain, 37.63°W), KEV (27.01°E), KIL (20.87°E) and LOZ (northern Russia, 35.02°E) are plotted in the upper panel. LOZ is located slightly eastward of the IMAGE stations and clearly outside of the breakup current system. However, the LANL measurements further east of LOZ indicate that the injection region had a much wider longitudinal extent. To the west, the breakup did not reach the east coast of the Greenland and thus, this event was limited in a few MLT hours. According to IMAGE magnetograms, the latitudinal scale of the activation was only about 4°. The dispersion time of the drifting hole, as measured by LANL, was 1.5–2.0 min from the lowest (50–75 keV) to the second highest (0.75–1.1 MeV) energy channel. This time delay together with the typical drift velocities of electrons in the two energy ranges (assuming 90° pitch angle) suggests that the origin of the injection took place about 8–11° east of the satellite. Scandinavia is not yet directly under this area, but as reported by Reeves *et al.* [1990] and Reeves *et al.* [1991] the injection regions at the geostationary orbit are often much wider (up to ~90° around the midnight) than the ionospheric current system would suggest.

3.3. Electrodynamics of the Pseudo-Breakup Spiral

[23] Top panel of Figure 5 shows the evolution of the spiral over KIL at 2211–2213 UT. The spiral at 2212 UT as observed by the MUO and KIL ASCs is reproduced in the bottom panel of Figure 5 by applying the inversion method

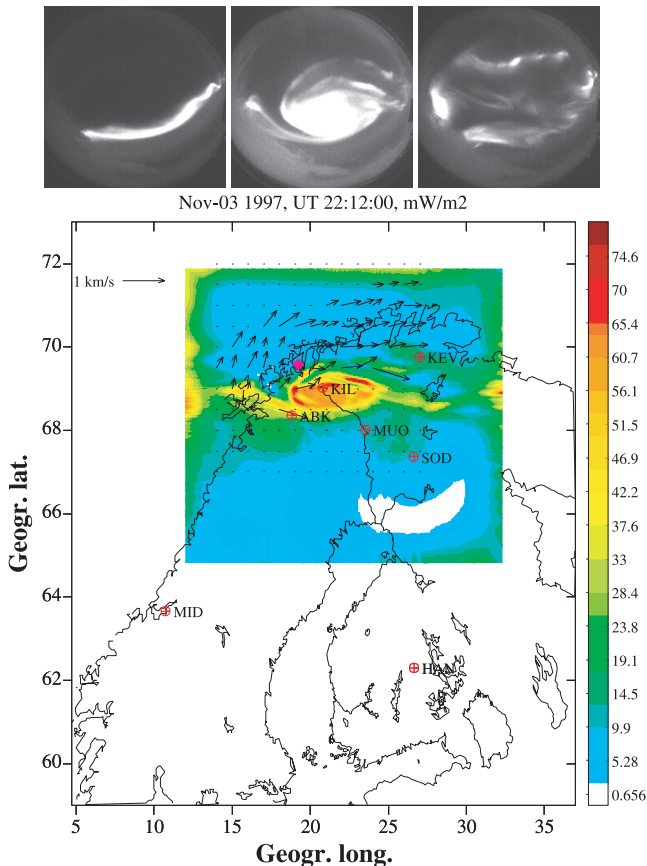


Figure 5. The top panel shows the evolution of the auroral spiral as a sequence of the KIL ASC images at 2211:00 UT (left), 2212:00 UT (middle) and 2213:00 UT (right). Plotted are the inversed ASC images together with the plasma flow field from STARE. In the inversion both green (557.7 nm) and red (630.0 nm) light images from KIL and MUO are used, and an altitude of 100 km is assumed in mapping. The pink diamond marks the EISCAT Tromsø site.

of *Janhunen* [2001] to the green and red light images. The inversion method takes into account the altitude structure of the auroras and thus, provides a better mapping than plain conversion to geographic coordinates. Compared to the observed aurora (top panel in Figure 5), the inverted spiral form is well reproduced and also some filamentary fine structures are visible. As the MIRACLE ASCs were not yet calibrated in 1997, the absolute energy flux values given in Figure 5 are estimates only. Furthermore, the saturation of the ASC images prohibit us from seeing the changes in the highest intensities. The overlaid vectors show the horizontal plasma velocity field measured by the STARE radars. The velocity was northward to the west of the spiral and turned gradually being eastward to the north of the spiral. No measurements were available within the aurora, because the conductivities were high in the precipitation region and thus, the electric fields decreased below the radar measuring threshold. The southern and southeastern parts of the auroral structure were outside the radar FOV, which explains the lack of measurements in those regions. However, the flow pattern suggests a clockwise plasma flow in the spiral surroundings. This rotation is opposite to the counterclock-

wise winding of the spiral, but consistent with the $\mathbf{E} \times \mathbf{B}$ drift in a region of upward FAC and converging electric fields.

[24] The method of characteristics [*Amm*, 1998] uses the electric field measured by STARE and IMAGE magnetic field data as inputs together with an estimate of the ratio of Hall to Pedersen conductivity α . Here α is assumed to be 3 at latitudes 68° – 69° , and 1.5 at latitudes 69° – 71.5° . The model outputs are the distribution of the Hall conductivity, horizontal Hall and Pedersen currents, field-aligned currents (FAC) due to both Hall and Pedersen currents, as well as the total FAC. The spatial resolution of the method is about 50 km ($\sim 0.5^\circ$) in latitude and 200 km ($\sim 2.0^\circ$) in longitude, i.e., of the size of the spiral. Within these resolutional limits the method of characteristics has been shown to be reliable (for a detailed discussion on the error estimates, see *Amm* [1995]). The total FAC distribution at 2211:40 UT is presented in Figure 4. The region of the strongest downward FACs is found to the northeast of the auroral spiral. The most intense upward FACs are located to the east and west of the spiral, about 1° south of the downward FAC region. Only weak downward directed currents are colocated with the spiral. In the spiral region the FACs of scale sizes smaller than the spatial resolution of the method sum up to an almost zero net current. Both regions of strong upward FACs were colocated with the areas of most intense Hall conductance gradients (Figure 6). The peak value of the Hall conductance is 40 S within the spiral and the strongest gradients appear westward of the spiral. Similar conductivity values have also been recorded during full-scale substorms [*Gjerloev and Hoffman*, 2000].

[25] The conductivities were also estimated from the EISCAT Tromsø radar measurements (location is marked in Figure 6) using a program called Spectrum (for more details, see *Kirkwood* [1988]). This program utilizes the Neutral Atmosphere Empirical Model (MSISE90) [*Hedin*, 1991] for calculating the collision coefficients. The resulting height-integrated Hall conductance at 2212 UT along the radar beam is about 2.6 S, and the corresponding value from the method of characteristics is 20–25 S. The auroral form has a fairly sharp boundary toward the radar (north) but for the method of characteristics the sharpness of the boundary is limited by its latitudinal resolution of 50 km. Thus, the high conductances within the aurora are smeared out at the edges causing the discrepancy between the EISCAT observations and the values in Figure 6. Furthermore, when the precipitation reached the radar beam at 2215 UT, the EISCAT conductances grow rapidly to the values (25–27 S) comparable to the peak values of the model (40 S).

[26] The total horizontal currents (Figure 7) are dominated by the southwest directed Hall currents. The Pedersen currents cause only a slight counterclockwise rotation of the current vectors at the poleward edge of the spiral. The total current field supports the pattern of a local current closure being directed from the downward to the upward FAC region. Unlike a typical east-west aligned (along the oval) substorm current wedge, the current in our case is flowing across the narrow oval in the northeast-southwest direction. In the region of interest the sum of the upward and downward FACs is 671 kA and 505 kA, respectively. Thus, the

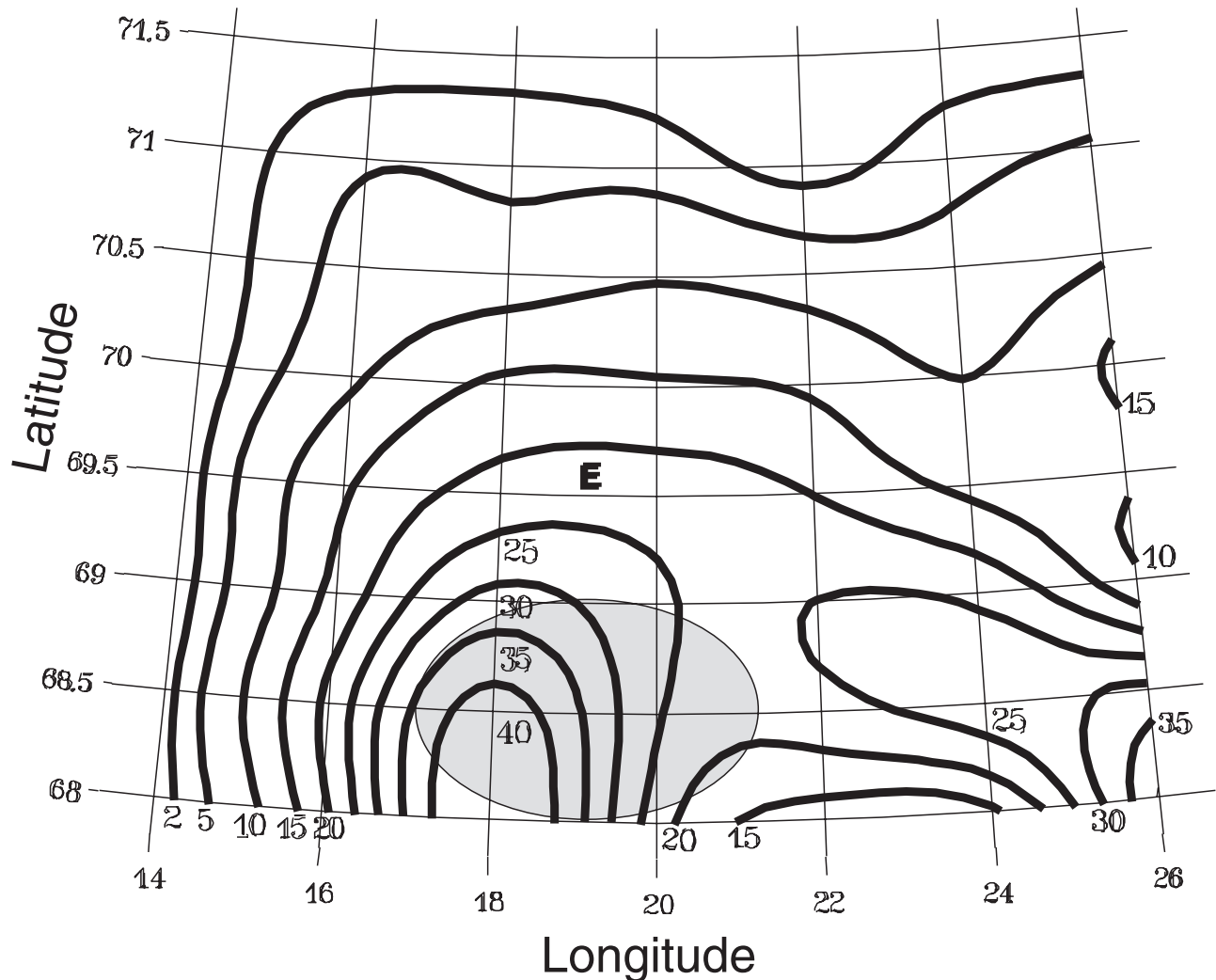


Figure 6. Distribution of the Hall conductance (S) at 2212 UT as a result of the method of characteristics. The shaded area shows the spiral location and size. The location of the EISCAT TRO radar (69.58°N, 19.23°E) is marked by a letter E.

FAC system closed locally within this region. The maximum current density at the western edge of the spiral was ~ 6 A/km², which clearly exceeds the threshold of the spiral formation (2.5 A/km²) suggested by the theoretical study of Hallinan [1976].

4. Discussion

4.1. Comparisons With Other Pseudo-Breakup Events

[27] In the event analyzed by Amm *et al.* [2001] the pseudo-breakup lasted roughly 3 min and occurred in the midnight sector, westward of the main activity region. Similarly to the event studied here, the pseudo-breakup took place poleward of the following substorm. The FACs and horizontal currents derived with the method of characteristics [Amm, 1995] did not form a local current closure like in our case, but the upward FACs in the pseudo-breakup region were closed by remote FACs outside and eastward of the analysis area. The region of the strongest upward FAC located at the northern boundary of the auroral vortex structure, while the strongest conductivity gradients were

found west of the aurora, just like in the event studied here. Since the IMF B_z had been negative for an extended period and there was ample energy in the magnetosphere, and the ionospheric conductivity was high enough for a substorm, the authors concluded that some features in the internal magnetospheric conditions prevented the activation from growing to a global substorm expansion phase. Also in our case the ionospheric conductivity at the pseudo-breakup onset was high enough for a full-scale substorm. The energy input from the solar wind stayed above 10^{11} W [Akasofu, 1981] for about an hour before the activation, but dropped down to $0.4 \cdot 10^{11}$ W at its onset. According to Kallio *et al.* [2000], the solar wind energy input during the expansion phase controls the intensity of the activation. After the pseudo-breakup onset the input was very small and thus the activity ceased. On contrary, during the following substorm the ϵ values increased and as a result a global-scale substorm took place. The location of our pseudo-breakup event in the postmidnight sector was probably another crucial factor prohibiting the activation to reach global extent. According to the coupled two-circuit magneto-

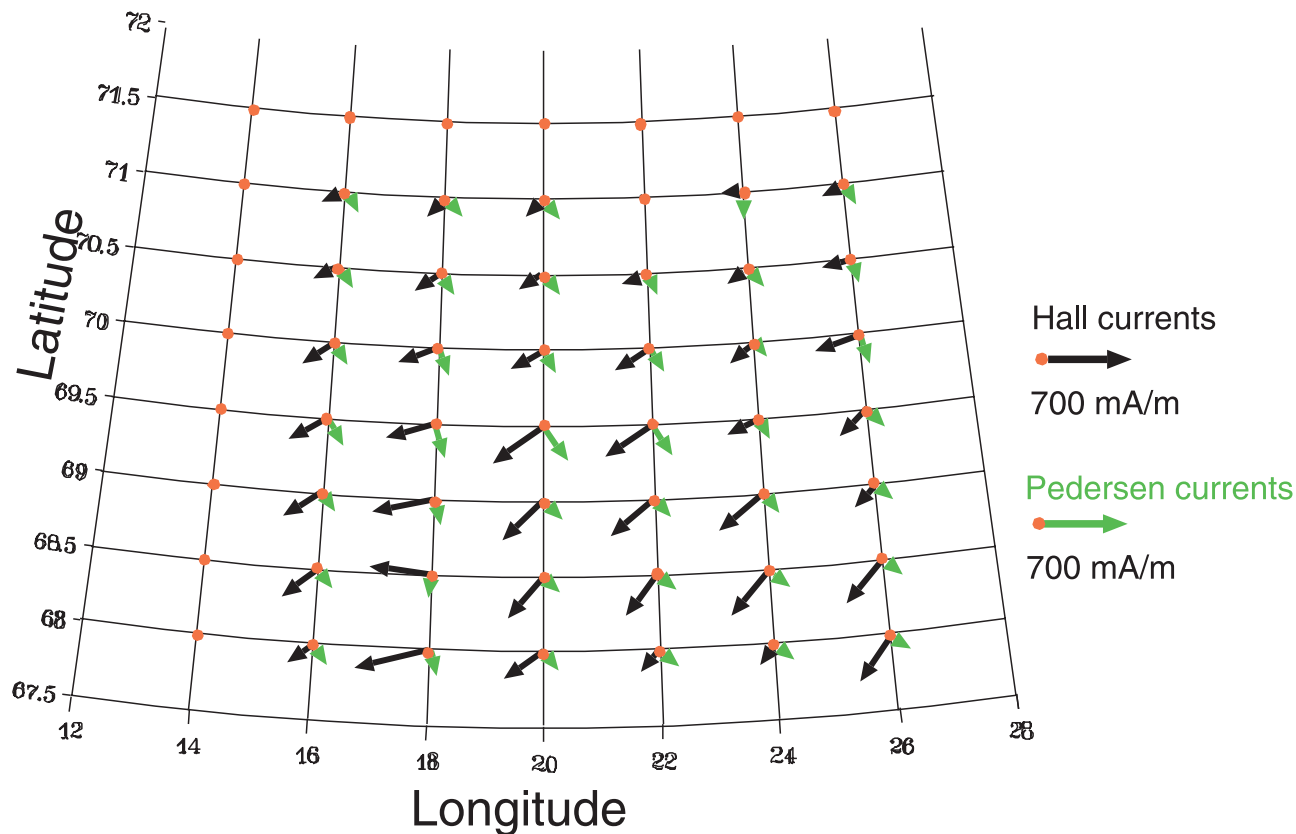


Figure 7. Horizontal Hall (black) and Pedersen (green) current vectors as produced by the method of characteristics.

sphere-ionosphere coupling model of pre-breakup arcs by Rothwell *et al.* [1991], magnetospheric plasma flows in the postmidnight sector are not as efficient FAC generators as flows in the evening sector.

[28] A similar situation has been discussed by Yahnin *et al.* [1983] in a study of a weak (~ 70 nT), short-lived (~ 6 min) and localized (~ 250 km in latitude and ~ 1 hour in MLT) substorm, which took place within the region of westward electrojet. Also this activation was preceded by a period of negative IMF B_z , and during the event the IMF B_z turned northward. The authors consider the IMF turning as an external impulse trying to trigger the substorm activity when the magnetotail did not meet the conditions for a large-scale instability.

[29] The localized current wedge of our event resembles the current systems observed by Baumjohann *et al.* [1981] during a sequence of substorm intensifications. The activations were localized in latitude (some 100 km), longitude (roughly 1000 km) and time (less than 10 min), and the deviations in X-component as well as the estimated ionospheric conductivities were of the same order as in our case. However, the local wedges of the activations were systematically aligned in east-west direction. Only about one fourth of the horizontal currents were directed northward and closed by the FACs at the northern and southern boundaries of the active region. Thus, our observation of a wedge aligned rather across the oval than along it is different from the previously studied pseudo-breakup type events.

[30] From the viewpoint of geostationary particle flux data, our event is not exceptional. Yahnin *et al.* [2001] also reported about drifting electron holes in their study of a “pseudo-breakup phase” of an isolated substorm. Our event could be considered as a “pseudo-breakup phase” with only one activation. However, as our event was observed also by riometers, we do not believe that the poor energization of the magnetospheric particles would explain the decay of the activation like Yahnin *et al.* did. Also Koskinen *et al.* [1993] considered the weakness of the magnetospheric energization processes to be the main reason for the quenching of the pseudo-breakup. Although their pseudo-breakup event was associated with a weak geostationary particle injection it did not cause any signatures in riometer data.

4.2. Connection to the IMF B_z Turning?

[31] The timing of the pseudo-breakup event of this paper suggests its association with the northward turning of the IMF B_z . According to the simplest estimate of the propagation delay of the IMF change from the satellite to the magnetopause ($T_{LAG} = (X_{Wind} - 10 R_E)/V_{SW}$, where X_{Wind} is the X-component of the Wind position in GSE and V_{SW} is the average solar wind speed observed by the satellite), the ionospheric response on the nightside would have been simultaneous with the arrival of the IMF turning to the subsolar magnetopause with the time delay of $T_{LAG} = 31$ min. This time lag was also obtained as a result of a cross-correlation between the IMF B_z and the magnetic X-

component measured at KIL with a correlation coefficient of 0.86. The ACE and IMP-8 satellites were also in the solar wind during the period of our interest. ACE was further away from the Earth ($X_{GSE} \sim 220 R_E$) and the Sun-Earth line ($Y_{GSE} \sim -70 R_E$) but closer to the XY-plane ($Z_{GSE} \sim 2 R_E$) than Wind. About 37 min earlier than Wind it recorded IMF variations almost identical to those measured by Wind, including also the IMF northward turning that matches the pseudo-breakup timing. This time difference of 37 min is consistent with the observed solar wind speed and the distance ($\sim 110 R_E$) between the satellites. The IMP-8 satellite was much closer to the magnetopause ($X_{GSE} \sim 35 R_E$, $Y_{GSE} \sim 20 R_E$, $Z_{GSE} \sim -20 R_E$) but the data were available only until 2130 UT. Although it did not record the IMF turning, all the earlier variations were similar to the Wind recordings with a time delay of about 26 min (distance of $\sim 85 R_E$). Thus all the satellite measurements are in a good agreement with the 31-min time delay between the Wind satellite and the ground-based observations.

[32] However, estimating the propagation time of the solar wind structures from upwind satellites to the magnetopause is not a straightforward task and does not necessarily give accurate results. As suggested by *Collier et al.* [1998], the uncertainty in the propagation time (ΔT) is strongly dependent on the satellite's position in the solar wind, and can be estimated by the equation

$$\Delta T \sim (D_{\perp}/D_{\parallel}) \cdot T_{LAG} \quad (1)$$

where D_{\perp} is the distance between the Sun-Earth line and the satellite and D_{\parallel} is the distance of the satellite from the magnetopause. Using the GSE coordinates of Wind, we obtained the timing uncertainty of about 17 min. The corresponding timing uncertainty for the ACE satellite is 23 min. These errors in timing are comparable to the ionospheric response times to subsolar IMF changes (15–20 min) reported by *Cowley and Lockwood* [1992].

[33] Keeping in mind the timing uncertainty of about 17 min in the delay time from Wind to the magnetopause, we checked the SuperDARN [*Greenwald et al.*, 1995] radar data and recordings from several magnetometer networks from 2155 UT until 2230 UT to find ionospheric signatures of the IMF B_Z turning. No effects were found in the dayside magnetograms of the 210 MM and CANOPUS networks (~ 07 MLT and 14–16 MLT, respectively), or the stations inside the polar cap (THL in Greenland and VOS in the Antarctic). Examination of line-of-sight velocities of individual SuperDARN radars did not reveal any obvious response signatures either. Iceland East radar monitors mainly the plasma flows along the oval in the Scandinavian sector. During 2200–2210 UT the radar observed continuous westward flows (with velocities of 200–400 m/s) in the polar cap region (data not shown here), which is consistent with the morning cell convection. Simultaneous IMAGE magnetometer observations (cf. Figure 3) of the westward electrojet at the auroral latitudes further support this conclusion. At 2212 UT the radar backscatter dropped abruptly, which is probably a consequence of a change in the radar viewing conditions due to increased E-layer conductivities caused by enhanced precipitation. The time resolution of these observations is 2 min and thus, we cannot determine

whether the decrease in radar echo preceded the pseudo-breakup or not.

5. Conclusions

[34] We have given a detailed description of a pseudo-breakup event on 3 November 1997, with a good coverage of ground-based instrumentation and solar wind observations. The pseudo-breakup took place during a substorm growth phase. Both the Wind and ACE data suggest that the IMF B_Z turned toward positive values at the subsolar point at the pseudo-breakup onset time. The errors in the time delay from the spacecraft to the magnetopause, according to *Collier et al.* [1998], are 23 min for ACE and 19 min for Wind, i.e., comparable with the previously reported signal propagation times from the magnetopause to the nightside ionosphere [*Cowley and Lockwood*, 1992]. However, besides the pseudo-breakup, neither SuperDARN data nor polar cap or dayside magnetometer data showed any signatures of the IMF turning within the time windows defined by the timing uncertainties. Thus, the hypothesis associating the IMF B_Z northward turning with the pseudo-breakup onset remains without profound observational confirmation.

[35] In the ionosphere, the pseudo-breakup aurora formed a counterclockwise spiral structure with clockwise plasma flow in the same region. The method of characteristics [*Amm*, 1998] was used to determine the distribution of ionospheric Hall conductivity and both horizontal and field-aligned currents. As a rough estimation of the total FAC balance in the area of interest, we summed separately the upward and downward FAC values. The result for the downward current is 671 kA and for the upward current 505 kA. This, together with the pattern of the horizontal currents, suggests that the FAC was mainly closed locally within our analysis region. The current system resembled much a substorm current wedge, although in this case the ionospheric part of the wedge was not east-west directed but rather northeast-southwest directed. The size of the wedge was about 4° in latitude and less than a few hours in MLT. The peak current density of the spiral exceeded the threshold value of the spiral formation suggested by *Hallinan* [1976]. The pseudo-breakup was associated with a drifting electron hole recorded by the geostationary LANL instrument 40° east from the region of ground-based observations. As the first approximation (drift of the 90 pitch angle particles), the observed energy dispersion of the hole corresponds to a source region only about 10° (instead of 40°) west of the satellite. Thus, the injection region at the geostationary distance seemed to be azimuthally much wider than the ionospheric current system. Indeed, the Russian magnetometer station in Lovozero, which is located between the regions of the ground-based and satellite observations, did not record any significant variations during the pseudo-breakup.

[36] Within the spiral structure, both EISCAT observations and the method of characteristics yielded Hall conductivity values high enough to allow a substorm current wedge formation. Also, the energy input from the solar wind to the magnetosphere (ϵ) exceeded the substorm threshold value of 10^{11} W about an hour before the pseudo-breakup, but then dropped down to about $0.4 \cdot 10^{11}$ W at the onset time. Consequently, the direct input

from the solar wind did not feed the activation like it often does during full-scale substorms [Kallio et al., 2000]. Furthermore, the unfavorable location of the activation in the morning side of the Harang discontinuity region probably prohibited it from becoming a global-scale substorm.

[37] **Acknowledgments.** The work by N.P. was supported by the Finnish Graduate School in Space Physics and Astronomy. We thank Geoff Reeves for the Los Alamos National Laboratory satellite data. The MIRACLE network is operated as an international collaboration under the leadership of the Finnish Meteorological Institute. The IMAGE magnetometer data are collected as a Finnish-German-Norwegian-Polish-Russian-Swedish project. EISCAT is an International Association supported by Finland (SA), France (CNRS), the Federal Republic of Germany (MPG), Japan (NIPR), Norway (NFR), Sweden (NFR) and the United Kingdom (PPARC). The PCN index was obtained from the WDC in Copenhagen. Sodankylä geophysical observatory is acknowledged for providing the Finnish riometer data. We also thank R. Lepping (NASA/GSFC) for the Wind MFI data, A. Szabo for the IMP-8 magnetic field data, C. W. Smith for the ACE magnetic field data, G. Parks for the Polar UVI data, L. A. Frank for the Polar VIS data, and O. A. Troshichev for the magnetic field data at Russian stations and in the Antarctic as well as the PCS index.

References

- Aikio, A. T., V. A. Sergeev, M. A. Shukhtina, L. I. Vagina, V. Angelopoulos, and G. D. Reeves, Characteristics of pseudobreakups and substorms observed in the ionosphere, at the geosynchronous orbit, and in the mid-tail, *J. Geophys. Res.*, **104**, 12,263–12,287, 1999.
- Akasofu, S.-I., The development of the auroral substorm, *Planet. Space Sci.*, **12**, 273, 1964.
- Akasofu, S.-I., Energy coupling between the solar wind and the magnetosphere, *Space Sci. Rev.*, **28**, 121, 1981.
- Amm, O., Direct determination of the local ionospheric Hall conductance distribution from two-dimensional electric and magnetic field data: Application of the method using models of typical ionospheric electrodynamic situations, *J. Geophys. Res.*, **100**, 21,473, 1995.
- Amm, O., Method of characteristics in spherical geometry applied to a Harang-discontinuity situation, *Ann. Geophys. Lett.*, **16**, 413–424, 1998.
- Amm, O., P. Janhunen, K. Kauristie, H. J. Opgenoorth, T. I. Pulkkinen, and A. Viljanen, Mesoscale ionospheric electrodynamic observed with the MIRACLE network, 1, Analysis of a pseudobreakup spiral, *J. Geophys. Res.*, **106**, 24,675–24,690, 2001.
- Baumjohann, W., R. J. Pellinen, H. J. Opgenoorth, and E. Nielsen, Joint two-dimensional observations of ground magnetic and ionospheric electric fields associated with auroral zone currents: Current systems associated with local auroral break-ups, *Planet. Space Sci.*, **29**, 431–447, 1981.
- Browne, S., J. K. Hargreaves, and B. Honary, An imaging riometer for ionospheric studies, *Electron. Commun.*, **7**, 209–217, 1995.
- Cattell, C., C. Roller, and R. Lopez, Multi-spacecraft observations of substorm onsets and precursor events, in *Substorms*, vol. 2, edited by J. R. Kan, J. D. Craven, and S.-I. Akasofu, p. 247, Geophys. Inst., Alaska, 1994.
- Collier, M. R., J. A. Slavin, R. P. Lepping, A. Szabo, and K. Ogilvie, Timing accuracy for the simple planar propagation of magnetic field structures in the solar wind, *Geophys. Res. Lett.*, **25**, 2509–2512, 1998.
- Cowley, S. W. H., and M. Lockwood, Excitation and decay of Solar wind-driven flows in the magnetosphere-ionosphere system, *Ann. Geophys. Lett.*, **10**, 103–115, 1992.
- Gjerloev, J. W., and R. A. Hoffman, Height-integrated conductivity in auroral substorms, 1, Data, *J. Geophys. Res.*, **105**, 215, 2000.
- Greenwald, R. A., W. Weiss, and E. Nielsen, STARE: A new radar auroral backscatter experiment in northern Scandinavia, *Radio Sci.*, **13**, 1021–1039, 1978.
- Greenwald, R. A., et al., DARN/SuperDARN, A global view of the dynamics of high-latitude convection, in *The Global Geospace Mission*, edited by C. T. Russell, p. 761, Kluwer Acad., Norwell, Mass., 1995.
- Hallinan, T. J., Auroral spirals, 2, Theory, *J. Geophys. Res.*, **81**, 3959–3965, 1976.
- Hedin, A. E., Extension of the MSIS thermosphere model into the middle and lower atmosphere, *J. Geophys. Res.*, **96**, 1159–1172, 1991.
- Janhunen, P., Reconstruction of electron precipitation characteristics from a set of multi-wavelength digital all-sky auroral images, *J. Geophys. Res.*, **106**, 18,505–18,516, 2001.
- Kallio, E. I., T. I. Pulkkinen, H. E. J. Koskinen, A. Viljanen, J. A. Slavin, and K. Ogilvie, Loading-unloading processes in the nightside ionosphere, *Geophys. Res. Lett.*, **27**, 1627–1630, 2000.
- Kirkwood, S., SPECTRUM—A computer algorithm to derive the flux-energy spectrum of precipitating particles from EISCAT electron density profiles, *IRF Tech. Rep. 034*, Swed. Inst. of Space Phys., 1988.
- Koskinen, H. E. J., R. E. Lopez, R. J. Pellinen, T. I. Pulkkinen, D. N. Baker, and T. Bsinger, Pseudobreakup and substorm growth phase in the ionosphere and magnetosphere, *J. Geophys. Res.*, **98**, 5801–5813, 1993.
- Nakamura, R., D. N. Baker, T. Yamamoto, R. D. Belian, E. A. Bering, J. A. Benbrook, and J. R. Theal, Particle and field signatures during pseudobreakup and major expansion onset, *J. Geophys. Res.*, **99**, 207, 1994.
- Ohtani, S., et al., A multisatellite study of a pseudo-substorm onset in the near-Earth magnetotail, *J. Geophys. Res.*, **98**, 19,355, 1993.
- Partamies, N., K. Kauristie, T. I. Pulkkinen, and M. Brittnacher, Statistical study of auroral spirals, *J. Geophys. Res.*, **106**, 15,415–15,428, 2001.
- Perreault, P., and S.-I. Akasofu, A study of geomagnetic storms, *Geophys. J. R. Astron. Soc.*, **54**, 547, 1978.
- Pulkkinen, T. I., Pseudobreakup or Substorm?, *Proc. Int. Conf. Substorms 3rd*, 285–293, 1996.
- Pulkkinen, T. I., et al., Pseudobreakup and substorm onset: Observations and MHD simulations compared, *J. Geophys. Res.*, **103**, 14,847, 1998.
- Reeves, G. D., T. A. Fritz, T. E. Cayton, and R. D. Belian, Multi-satellite measurements of the substorm injection region, *Geophys. Res. Lett.*, **17**, 2015–2018, 1990.
- Reeves, G. D., R. D. Belian, and T. A. Fritz, Numerical tracing of energetic particle drifts in a model magnetosphere, *J. Geophys. Res.*, **96**, 13,997–14,008, 1991.
- Rostoker, G., On the place of the pseudo-breakup in a magnetospheric substorm, *Geophys. Res. Lett.*, **25**, 217, 1998.
- Rostoker, G., J. C. Samson, F. Creutzberg, T. J. Hughes, D. R. McDiarmid, A. G. McNamara, A. Wallace Jones, D. D. Wallis, and L. L. Cogger, CANOPUS—A ground-based instrument array for remote sensing the high-latitude ionosphere during the ISTP/GGS program, *Space Sci. Rev.*, **71**, 743–760, 1995.
- Rothwell, P. L., M. B. Silevitch, L. P. Block, and C.-G. Flthammar, Pre-breakup arcs: A comparison between theory and experiment, *J. Geophys. Res.*, **96**, 13,967–13,975, 1991.
- Sergeev, V. A., T. Bösinger, R. D. Belian, G. D. Reeves, and T. E. Cayton, Drifting holes in the energetic electron flux at geosynchronous orbit following substorm onset, *J. Geophys. Res.*, **97**, 6541–6548, 1992.
- Syrjäsoo, M. T., et al., Observations of substorm electrodynamic using the MIRACLE network, *Proc. Int. Conf. Substorms 4th*, 238, 111–114, 1998.
- Torr, M. R., et al., A far ultraviolet imager for the international solar-terrestrial physics mission, *Space Sci. Rev.*, **71**, 329, 1995.
- Troshichev, O. A., N. P. Dmitrieva, and B. M. Kuznetsov, Polar cap magnetic activity as a signature of substorm development, *Planet. Space Sci.*, **27**, 217, 1979.
- Yahnin, A. G., V. A. Sergeev, R. J. Pellinen, W. Baumjohann, K. U. Kaila, H. Ranta, J. Kangas, and O. M. Raspopov, Substorm time sequence and microstructure on 11 November 1976, *J. Geophys. Res.*, **53**, 182–197, 1983.
- Yahnin, A. G., et al., Correlated Interball/ground-based observations of isolated substorm: The pseudobreakup phase, *Ann. Geophys. Lett.*, **19**, 687–698, 2001.
- Yumoto, K., et al., Globally coordinated magnetic observations along 210° magnetic meridian during STEP period, 1, Preliminary results of low-latitude Pc 3's, *J. Geomagn. Geoelectr.*, **44**, 261–276, 1992.

O. Amm, K. Kauristie, N. Partamies, T. I. Pulkkinen, and E. Tanskanen, Geophysical Research, Finnish Meteorological Institute, P.O. Box 503, FIN-00101 Helsinki, Finland. (kirsti.kauristie@fmi.fi; noora.partamies@fmi.fi; tuuja.pulkkinen@fmi.fi)